SAND2019-0386D

Integrated Geomechanics and Geophysics in Induced Seismicity: Mechanisms and Monitoring

Hongkyu Yoon (PI), Michelle Williams, K-Won Chang, Charles Choens J. Eric Bower, Moo Lee (PM)
Academic Alliance: Laura Pyrak-Nolte & Antonio Bobet (Purdue Univ.)

Precursors to Induced Seismic Event

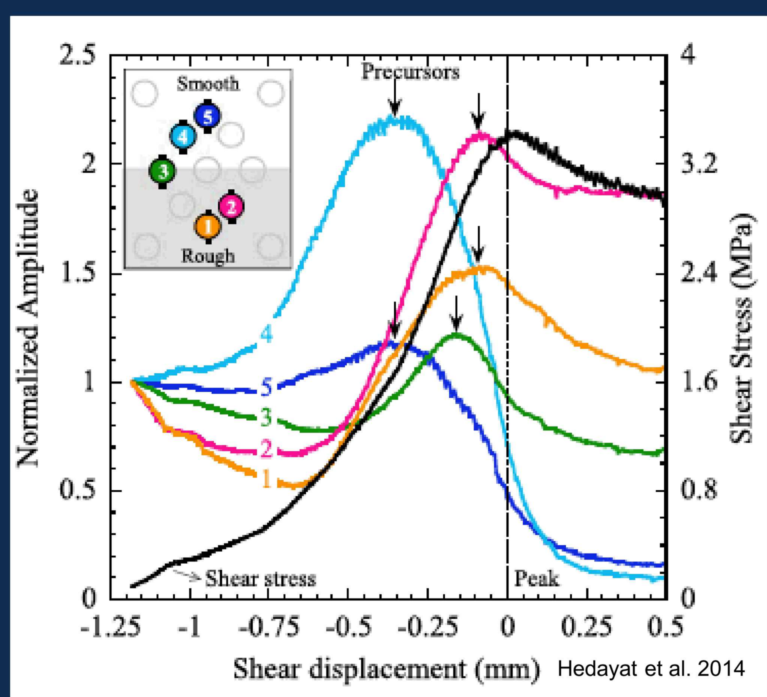

3D Printed Rock for Mechanical Testing

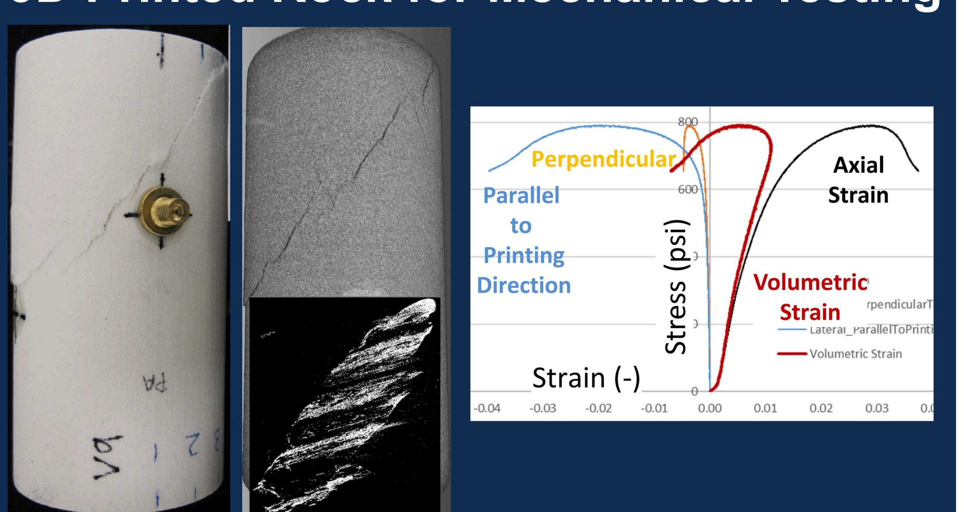

Poroelastic Response to Fluid Injection

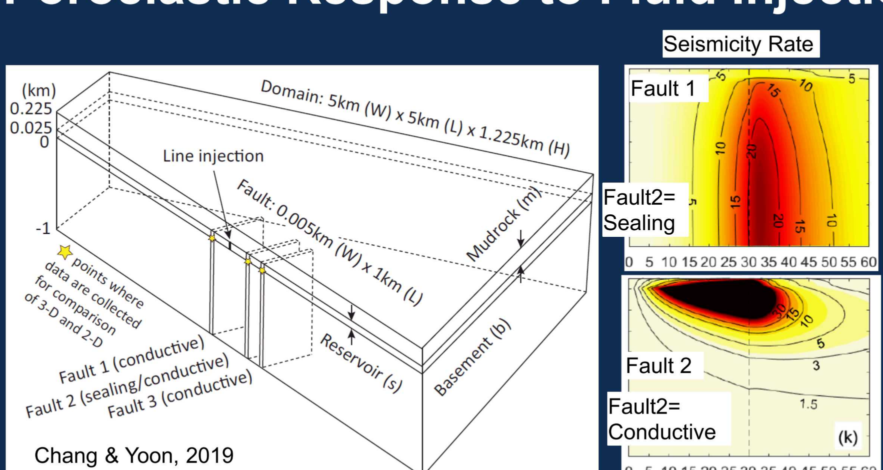

Numerical simulations of crack propagation & wave analysis

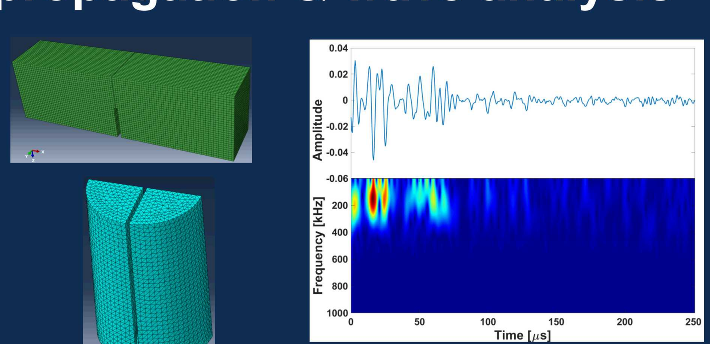

Science Challenges & Objectives

Challenges: Precursor(s) to the induced seismicity from existing fracture systems - linking mechanical discontinuities, fracture mechanics, pore pressures/stress to the geophysical signatures

Objectives: An ambitious integration of seismic imaging experiments coupled with micro-CT imaging, modeling of fracture initiation and propagation, and full waveform inversion will allow us to

(1) delineate crack initiation, propagation and failure using both active and passive seismic/ultrasonic monitoring techniques
(2) determine the poro-elastic coupling mechanisms that lead to induced seismicity during fluid injection into subsurface
(3) develop and implement automatic identification and interpretation of (micro-)seismic wave fields using machine-learning techniques

Induced seismicity

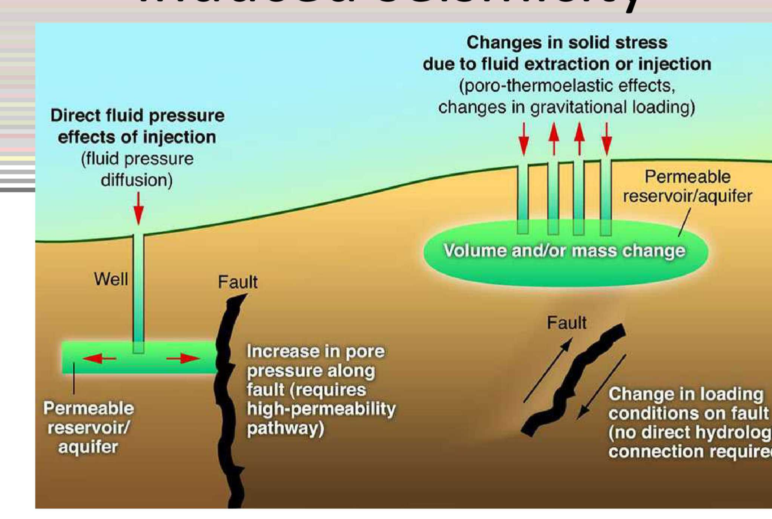

http://earthquake.usgs.gov/Research/induced/modeling.php

Fracturing testing and seismic signal acquisition

- Experimental specimens with multiple pre-existing flaws under dry/fluid-saturated P-T conditions - Natural rocks (Indiana Limestone)/ 3D printed
- Three point bending (3PB, top) and unconfined compressive strength tests (UCS, bottom) using a powder-based 3D printing technique

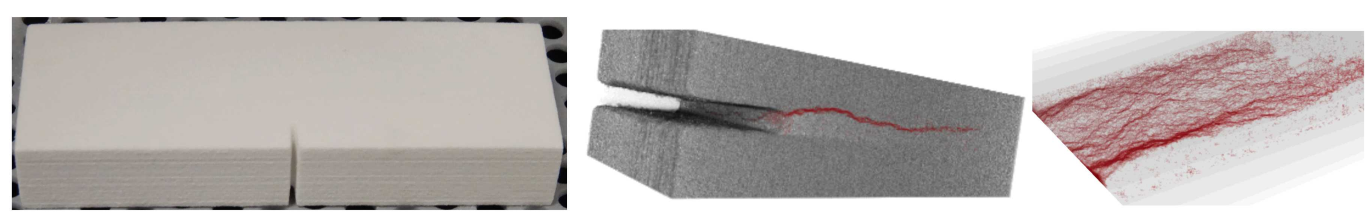

3D printing – Chemical reaction induced hardening process

$CaSO_4 \cdot 0.5H_2O + 1.5H_2O = CaSO_4 \cdot 2H_2O$

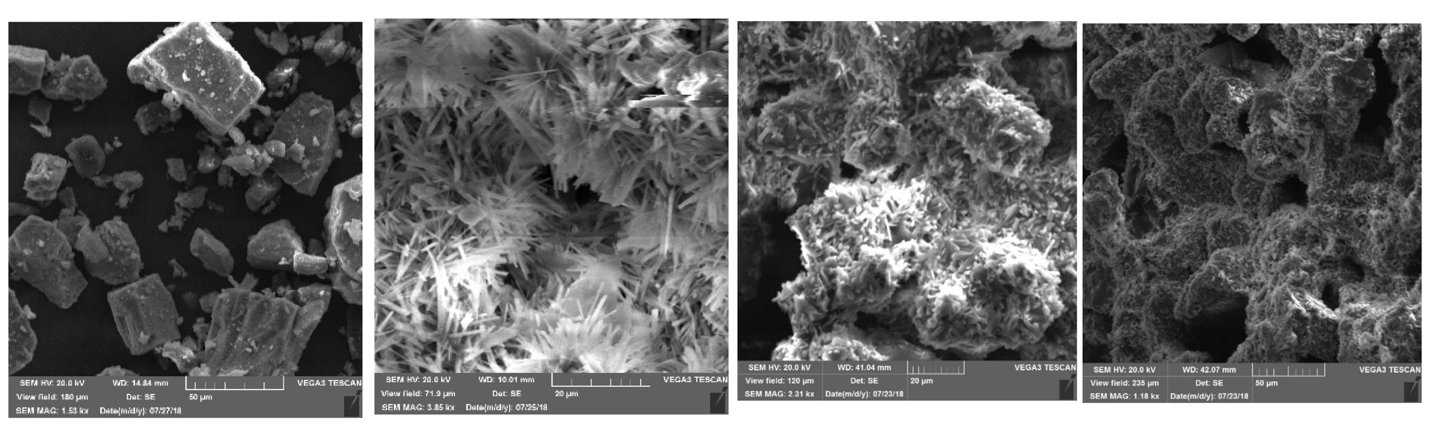

Powders (bassanite) Gypsum Gypsum/bassanite clusters

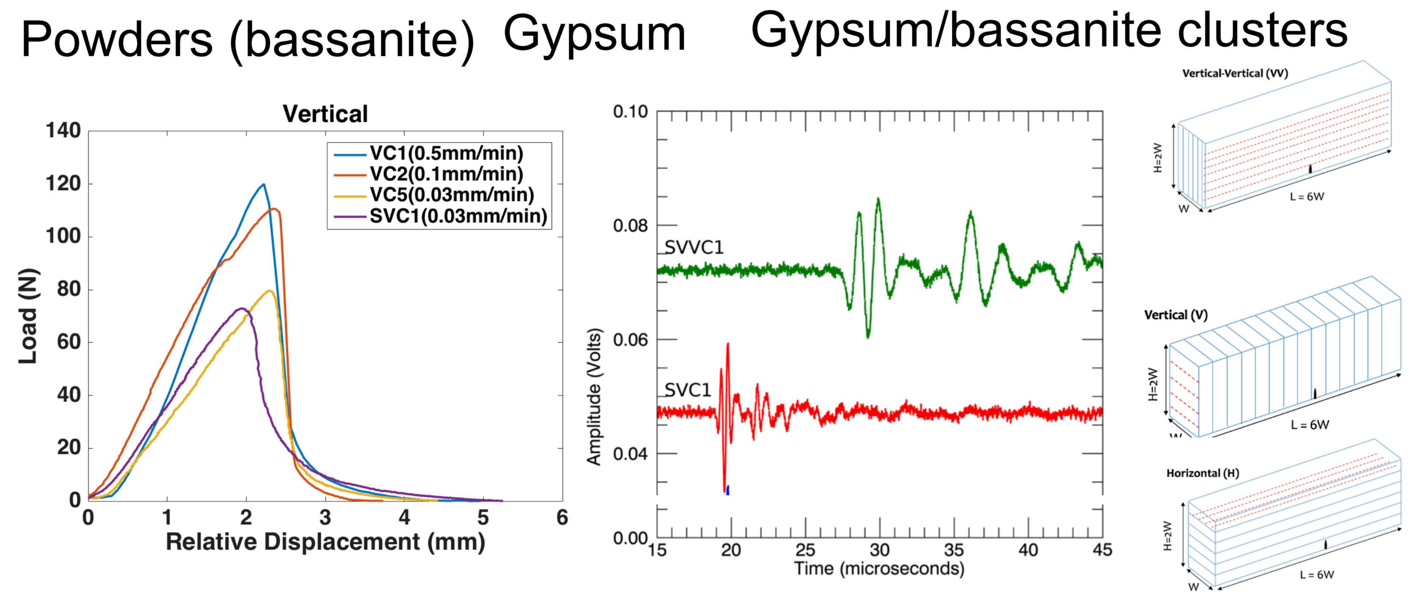

► Anisotropy in 3D printed rocks can rise from layering and direction of binder spray and mineral growth
► Peak loading, post-peak behaviors, fracture characteristics, and seismic signals during tensile & compressive failures are geometry-dependent
► Need to determine how these results apply in a more realistic setting with spatial and temporal variations in pre-existing discontinuities, stress and pressure fields, fluid migration and rock types

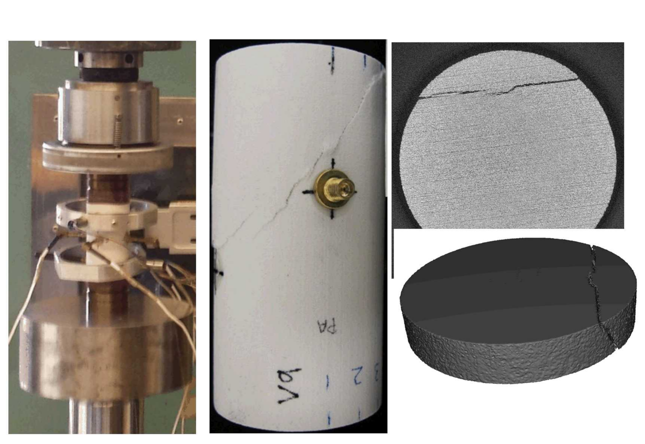

Original microCT image (left), segmented image of crack (WEKA in Fiji), and reconstructed 3D segmented image (right) for UCS tested sample

Poro-elastic coupling on injection-induced seismicity

- Stress equilibrium equation

$$\nabla \cdot [G(x)\nabla u] + \nabla \left[\frac{G(x)}{1-2\nu(x)}\right] \nabla \cdot u - \boxed{\alpha(x)\nabla p} + f = 0$$

- Inhomogeneous diffusion equation

$$S(x)\frac{\partial p}{\partial t} - \frac{1}{\eta}\nabla \cdot [k(x)\nabla p] = \boxed{-\alpha(x)\frac{\partial}{\partial t}(\nabla \cdot u)} + Q(x,t)$$

- Full poroelastic coupling is defined by ∇p in the equilibrium equation, acting as body forces in the stress equilibrium, and $\nabla \cdot u$ in the diffusion equation.

Coulomb stress change

$$\Delta\tau = \underbrace{(\Delta\tau_s + f\Delta\sigma_n)}_{\text{Poroelastic stress}} + \underbrace{f\Delta p}_{\text{Pore pressure}}$$

$\Delta\tau_s$ = shear stress change
$\Delta\sigma_n$ = normal stress change
Δp = pore pressure change
f = failure friction coefficient

- (+) values of each quantity imply that the fault plane is moved closer to failure

Seismicity rate estimate

$$\frac{dR}{dt} = \frac{R}{t_a}\left(\frac{\dot{\tau}}{\dot{\tau}_0} - R\right)$$

t_a = characteristic decaying time

- R is the seismicity rate relative to an assumed prior steady-state seismicity rate at a background stressing rate

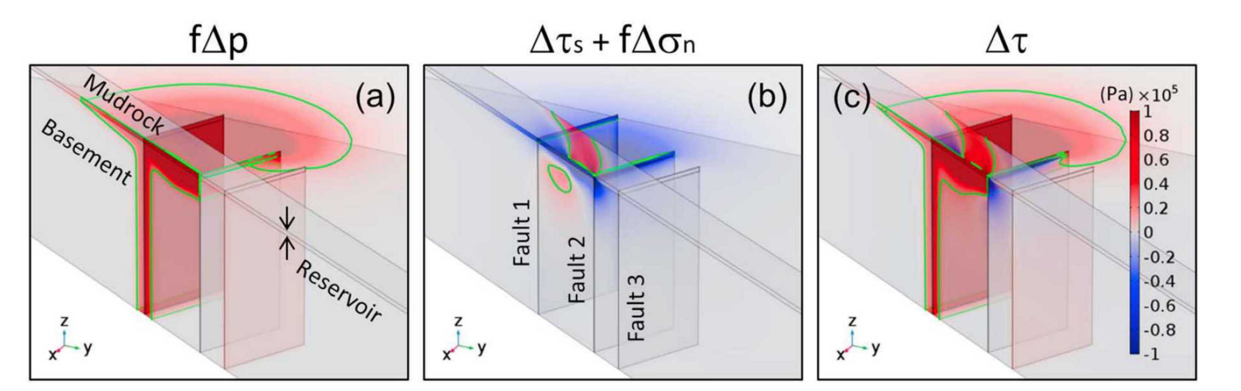

Figure 2. Spatial distributions of (a) pore pressure ($f\Delta p$), (b) poroelastic stress ($\Delta\tau_s + f\Delta\sigma_n$), and (c) Coulomb stress ($\Delta\tau$) at the end of injection ($t = 30$ days). Positive and negative changes are shown in red and blue, respectively. A contour line of 2×10^4 Pa is shown in each plot to clarify the spatial distribution of pore pressure and stresses.

- Pore pressure diffusion and/or poroelastic stressing induce seismicity along the fault with any hydraulic type
- The 3-D modeling captures properly the hydraulic and mechanical interaction between faults and surrounding formations, compared to 2D modeling

Numerical simulation, acoustic emission data analysis, & machine learning applications

- Crack propagation with cohesive element model & XFEM (ABAQUS) and acoustic emission (ABAQUS)
- FFT/STFT to create spectrogram (Cuadra, 2015)

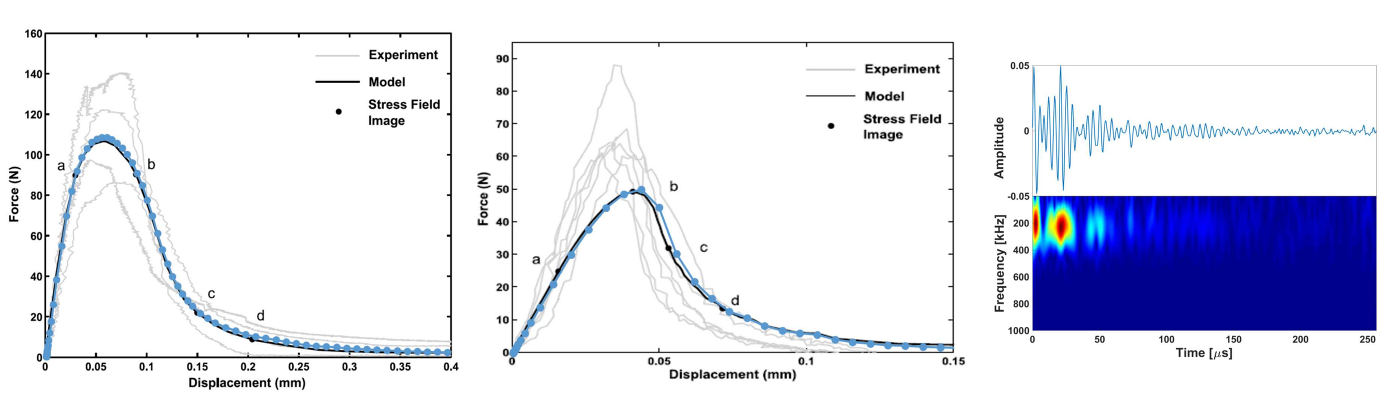

Acoustic emission during tensile cracking (left: 3PB; middle: short rod test) and associated spectrogram during 3PB (ABAQUS simulation result)

- Waveform similiarity-based event detection - Fingerprint and Similarity Thresholding (FAST) & Template matching
- Convolutional neural network for event detection and location
- Characterization of microseismic events during CO_2 injection at Illinois Basin Decator Project and enhanced geothermal testing at Pohang, Korea

- Chang, K. W., & Yoon, H. (2019). 3-D modeling of induced seismicity along multiple faults: Magnitude, rate, and location in a poroelasticity system. JGR, 123
- Hedayat, A., L. J. Pyrak-Nolte, and A. Bobet (2014), Seismic Precursors to the Shear Failure of Rock Discontinuities. Geophysical Research Letters, 41(15), 5467-5475
- Cuadra, 2015, A Computational Modeling Approach of Fracture-Induced Acoustic Emission, PhD thesis, Drexel University

Built on LDRD Laboratory Directed Research and Development

PURDUE UNIVERSITY

Sandia National Laboratories is a multimission laboratory managed and operated by National Technology and Engineering Solutions of Sandia LLC, a wholly owned subsidiary of Honeywell International Inc. for the U.S. Department of Energy's National Nuclear Security Administration under contract DE-NA0003525.
SAND No. 2019-XXXXP

U.S. DEPARTMENT OF ENERGY
NNSA National Nuclear Security Administration